

Metallic and semiconducting narrow carbon nanotubes

I. Cabria,¹ J. W. Mintmire,¹ and C. T. White²

¹*Department of Physics, Oklahoma State University, Stillwater, Oklahoma 74078-3072*

²*Naval Research Laboratory, Washington D.C. 20375-5320*

(Received 8 December 2002; published 20 March 2003)

We report local-density-functional results that show that narrow nanotubes with optimized diameters between about 0.34 and 0.5 nm can be either semiconducting or metallic, but with electron structures near the Fermi level that often cannot be understood starting from the graphene sheet model, successful in the study of larger diameter tubes. Our total-energy calculations indicate that narrow nanotubes recently observed either as the central shell of a multiwalled tube or encased in a porous zeolite, if isolated, should be stable against complete unzipping along the nanotube axis.

DOI: 10.1103/PhysRevB.67.121406

PACS number(s): 73.61.Wp, 73.22.-f, 71.15.Mb, 71.20.Tx

There has been good progress recently in producing carbon nanotubes with diameters smaller than the 0.7 nm diameter of icosahedral (I_h) C_{60} . These narrow nanotubes, with diameters in the range of about 0.33–0.50 nm, have been found either as the central shell of a multiwalled carbon nanotube,^{1,2} encased in the channels of a porous zeolite crystal,³ or perpendicularly anchored to the surface of larger nanotubes.⁴ The existence of even the narrowest of these nanotubes is consistent with the results of semiempirical molecular dynamics calculations that indicate that isolated single-walled carbon nanotubes (SWNT's) with diameters as small as 0.33 nm are mechanically stable to at least 1100 C, where vapor phase tube growth is thought to occur.⁴

All SWNT's can be indexed by a pair of integers associated with rolling up a graphene sheet along one of its two-dimensional lattice vectors $\mathbf{R} = n_1\mathbf{R}_1 + n_2\mathbf{R}_2$ to form a (n_1, n_2) cylindrical nanotube with radius r , where \mathbf{R}_1 and \mathbf{R}_2 are defined as in Fig. 1. A simple model of the electronic structure of these tubes is a Slater-Koster tight-binding model of the graphene sheet (characterized by the nearest-neighbor pp - π interaction, V_0), with periodic boundary conditions imposed over the rollup vector. This model, initially proposed based on results of first-principles calculations,⁵ and now supported by many experiments,^{6–12} has been used in successfully predicting many of the key properties of larger diameter carbon nanotubes.^{5,13–17} These properties include the grouping of SWNT's as either metallic or semiconducting,^{5,7,8,13,14} the linear dispersion relations of the metallic tubes in the vicinity of the Fermi level ε_F ,^{5,11,12,16} the r^{-1} dependence of the semiconducting band gaps,^{7,8,15} the stability of the metallic tubes against a Peierls distortion,⁵ and robust ballistic transport through metallic tubes.^{9,10,17}

Although the simple graphene sheet model (GSM) provides a good starting point for understanding the electronic properties of SWNT's with diameters similar to or greater than $I_h C_{60}$, much less is known about narrow nanotubes, where the effects of curvature can become more important.¹⁸ This lack of information has led to conflicting extrapolations from results for larger diameter SWNT's to the narrow carbon nanotubes. Thus, Qin *et al.*² and Wang *et al.*³ assume that nanotubes with diameters less than about 0.5 nm are generally metallic due to curvature, but Peng *et al.* assume

that the 0.33 nm SWNT they find anchored to a larger nanotube is a semiconductor, consistent with the neglect of curvature.⁴

We have calculated the electronic structure and equilibrium geometry of all narrow SWNT's with diameters between that of the (4,3) and (4,0) using a first-principles, all-electron, self-consistent local-density functional (LDF) band-structure method originally developed to treat chain polymers¹⁹ and especially tailored to take advantage of helical symmetry.²⁰ This method calculates the total energy and electronic structure using Gaussian-type orbitals within a one-dimensional (1D) band-structure approach. Our results predict that these narrow SWNT's can be either semiconductors or metals depending on their structure, but they cannot be grouped by the $3n$ rule applicable to larger diameter SWNT's.^{7,8,13–16,21} Although we find that the effects of curvature usually cause narrow SWNT's to have an electronic structure near the ε_F qualitatively different from that expected from the simple GSM, we also find that this is not always the case. Our calculations indicate that nanotubes with diameters as small as 0.382 nm are energetically stable and predict that the (4,3) has the largest band gap of all semiconducting SWNT's.

Every (n_1, n_2) SWNT can be generated by repeated applications of a screw operation S that translates and rotates a

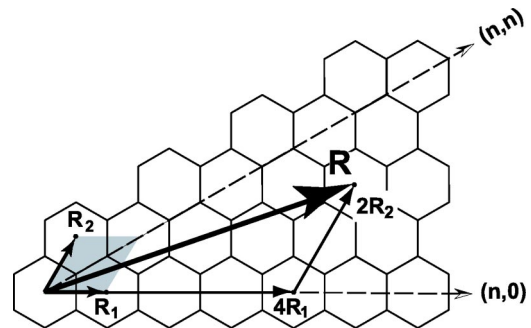


FIG. 1. 2D graphene lattice structure. Rollup vector \mathbf{R} for the narrow (4,2) SWNT is shown in terms of the primitive vectors \mathbf{R}_1 and \mathbf{R}_2 of the graphene sheet. Armchair nanotubes are defined by rollup vectors along the (n, n) direction; zigzag nanotubes are defined by rollup vectors along the $(n, 0)$ direction. A unit cell at the origin is highlighted in gray.

TABLE I. Equilibrium geometries and band gaps of narrow SWNT's obtained from the LDF calculations. See text for meanings of the geometric parameters.

(n_1, n_2)	$r(\text{nm})$	$\theta(\text{rad})$	$h'(\text{nm})$	$\phi(\text{rad})$	$h(\text{nm})$	Gap(eV)
(4,0)	0.171	$\pi/4^a$	0.073	$\pi/4^a$	0.213	metallic
(3,2)	0.180	0.821	0.017	2.480	0.050	0.46
(4,1)	0.191	0.749	0.048	4.935	0.047	metallic
(5,0)	0.206	$\pi/5^a$	0.073	π^a	0.215	metallic
(3,3)	0.212	0.699	0^a	π^a	0.125	metallic
(4,2)	0.217	0.672	0.028	5.159	0.081	0.34
(5,1)	0.228	0.608	0.052	5.168	0.039	0.00
(6,0)	0.245	$\pi/6^a$	0.073	$\pi/6^a$	0.215	metallic
(4,3)	0.246	0.593	0.012	1.783	0.036	1.28

^aFixed value.

primitive helical motif containing only a small number of atoms.¹⁵ Because the symmetry group generated by S is isomorphic with the 1D translational group, Bloch's theorem can be generalized so that the one-electron wave functions will transform under S according to $S^m \psi_i(\kappa) = e^{i\kappa m} \psi_i(\kappa)$.²⁰ The quantity κ is dimensionless and conventionally restricted to the central 1D Brillouin zone, $-\pi < \kappa \leq \pi$. The one-electron wave functions are then constructed from linear combinations of these helically adapted Bloch functions, which in turn are constructed from linear combinations of nuclear centered products of Gaussians and real solid spherical harmonics. This approach has already been successfully used in wide ranging studies of larger diameter SWNT's.^{16,22} To obtain the LDF results presented below, we adopted a $7s3p$ Gaussian basis set for carbon and assume 60 evenly spaced κ points over the central 1D Brillouin zone in solving the self-consistent LDF equations.

To optimize the geometries of the narrow SWNT's, we started from the corresponding unrelaxed nanotubes constructed by rolling up a graphene sheet. In rolling up the sheet, we assumed that the underlying honeycomb lattice had a C—C bond distance d of 0.144 nm, chosen based on ear-

lier optimizations for the (5,5) SWNT.²³ The geometries of the tubes were defined in terms of five scalar parameters: r , θ , h' , ϕ , and h . For the unrelaxed tubes, the first three of these parameters (r , θ , and h') define the positions of the two carbon atoms in a unit cell of graphene, such as that highlighted in gray in Fig. 1, when mapped (rolled) to the surface of the tube. The first atom in this unit cell can be thought of as mapped to an arbitrary point on the surface of a cylinder of radius r , with the second atom located relative to it by rotating an angle θ about the cylinder axis followed by a translation h' along this axis. All SWNT's have a C_N rotational axis which coincides with the cylinder axis, where N is the largest common divisor of n_1 and n_2 . Hence, the positions of these first two atoms can be used to locate $2(N-1)$ additional atoms on the cylinder surface by $(N-1)$ successive $2\pi/N$ rotations about this axis. Altogether, these $2N$ atoms complete the specification of a primitive helical motif. The SWNT can then be generated by repeated application of a screw operation $S(\phi, h)$ that translates this motif a distance h down the nanotube axis in conjunction with a rotation ϕ about this axis.

For the unrelaxed tube the five parameters (r , θ , h' , ϕ ,

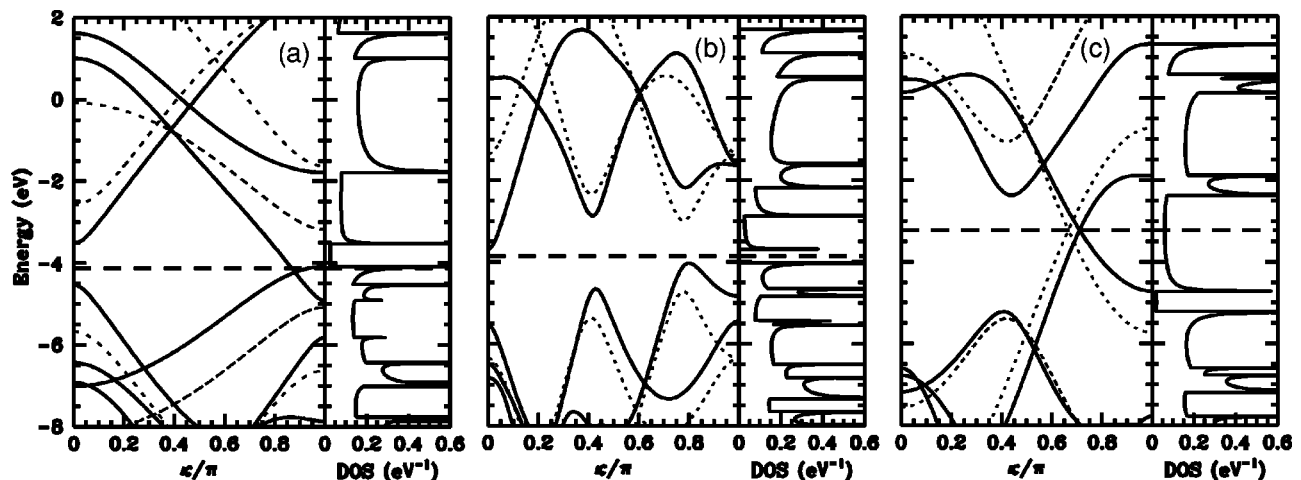


FIG. 2. LDF band structure and DOS for a series of similar diameter narrow SWNT's at the equilibrium geometry of Table I, including: (a) (5,0), (b) (4,2), and (c) (3,3) nanotubes. Also shown as broken lines are the corresponding band structures from the simple GSM obtained by assuming $V_0 = -2.5$ eV and aligning ϵ_F with the LDF values shown as horizontal dashed lines.

and h) can be easily expressed in terms of n_1 and n_2 .¹⁵ Starting from these unrelaxed values, the optimized values given in Table I are then obtained by minimizing the energy of the tube with respect to their variations. By construction this procedure maintains the helical and rotational symmetries of these tubes but not necessarily their translational symmetry.

First, focus on the subset of zigzag tubes in Table I and consider the (6,0), which has already been studied by Blase *et al.*¹⁸ Within the GSM the (6,0) is predicted to be metallic. However, contrary to the assumptions of this model, this and all other $(n,0)$ SWNT's should have two different C—C bond lengths: one corresponding to bonds oriented along the tube axis and the other corresponding to the remaining off-axis bonds. Once this effect is taken into account, the $(n,0)$ SWNT's, with n being a multiple of three, are found to be quasimetallic with small band gaps^{13,21} that scale as r^{-2} .^{24,25} Indeed, this scaling has been confirmed experimentally starting with tubes as narrow as the (9,0).²⁶ Table I shows, however, that rather than being quasimetallic, the (6,0) is actually metallic. Our calculated band structure at the equilibrium geometry does exhibit a small gap near ε_F which would have separated occupied from unoccupied states, if it were not for a partially occupied singly degenerate band. This band is also present in the graphene sheet and all-valence tight-binding (6,0) band structures, but in those cases completely empty because of the neglect of longer range interactions including those across the tube. These results are consistent with the original studies of Blase *et al.*¹⁸

Unlike the (6,0), the smaller diameter (5,0) and (4,0) SWNT's are semiconductors within the GSM, with band gaps exceeding an eV for reasonable choices of the nearest-neighbor pp - π interaction, V_0 .¹⁶ The results of Table I show, however, that these zigzag SWNT's should also be metallic. Again, this occurs because a singly degenerate band is lowered enough by interactions across the tube to convert these SWNT's to metals. This band can be seen in Fig. 2(a), where the LDF band structure and density of states (DOS) for the (5,0) SWNT are depicted. Such a singly degenerate band occurs in all $(n,0)$ SWNT's, but for quasimetallic tubes as narrow as the (9,0) lies too high in energy to affect the states near ε_F .

Based on the results for the narrow zigzag SWNT's, it might be tempting to conclude that all narrow SWNT's are metallic. However, this is not the case. Indeed, the results of Table I when combined with those from earlier first-principles studies of larger diameter SWNT's,^{16,22} imply that the (4,3) SWNT has the largest band gap of all possible SWNT's. In addition, for a reasonable choice of V_0 , the calculated band gap for this tube is close to that predicted from the expression $E_g = |V_0|d/r$ obtained from the simple GSM by ignoring the effects of trigonal warping.^{15,16}

The (4,2) and (3,2) SWNT's also have appreciable band gaps. Like the (4,3), both of these tubes are also predicted to be semiconductors within the GSM, but unlike the (4,3), their band gaps cannot be estimated from this model. Also, unlike the (4,3), the character of the HOMO-LUMO pair determining their band gaps is far different from what would be predicted from the GSM. This is illustrated in Fig. 2(b),

where the LDF and GSM band structures for the (4,2) SWNT are depicted. If the GSM were applicable, then the (4,2) would be a direct band-gap semiconductor with a gap approximately 15% larger than the (4,3). However, Fig. 2(b) and Table I show that the (4,2) is an indirect band-gap semiconductor,²⁷ with a gap approximately 75% smaller than the (4,3).

Finally, consider the (3,3) SWNT that is the only armchair tube among the set of narrow nanotubes treated in Table I. The LDF band structure and DOS for this tube at the optimized geometry of Table I are given in Fig. 2(c). The optimized radius of this tube is 0.21 nm, close to that reported by Qin *et al.*² As can be seen from Fig. 2(c), this tube has a first-principles electronic structure in the immediate vicinity of the ε_F similar to that predicted from the GSM, with two bands of different symmetry crossing approximately 2/3 across the zone and ε_F pinned at this crossing. Also, the magnitudes of the Fermi velocities corresponding to these two bands are similar. Of course, due to the effects of curvature the bands do not cross exactly at $\kappa = 2\pi/3$ and the magnitude of their slopes at ε_F are not identical. In addition, the positions of the peaks in the DOS nearest to ε_F differ from what would be expected based on the GSM.^{22,28} Nevertheless, Fig. 2(c) shows that the GSM does provide a good starting point for understanding the electronic structure of this narrow metallic SWNT in the immediate vicinity of ε_F . However, in comparison to larger diameter (n,n) tubes, the (3,3) should be far more susceptible to a spontaneous symmetry breaking that could convert it into a semiconductor.⁵ Thus, if the narrow (3,3) armchair SWNT

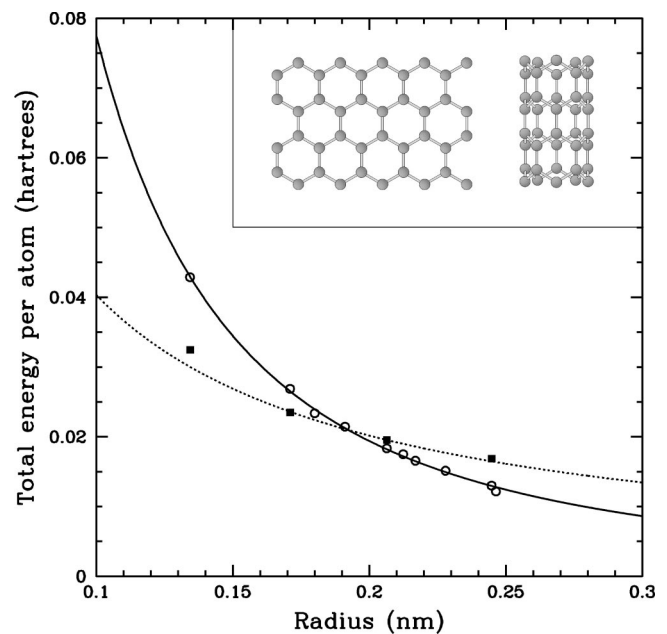


FIG. 3. Normalized strain E_s (circles) and edge E_e (black squares) energies of narrow SWNT's, with E_s fit to C/r^2 with $C = 0.021$ eV nm² and E_e fit to b/r with $b = 0.110$ eV nm; $r = r_c$ when the curves intersect. Points for E_s are for the tubes of Table I plus a relaxed (3,0). Points for E_e are for the $(n,0)$ tubes with $n = 3-6$. Inset shows a couple unit cells of a strip and corresponding (5,0) tube segment.

could not only be made but also isolated, it would be worthwhile to search for a Peierls gap and any accompanying topological excitations.

Table I shows that SWNT's as narrow as the (4,0) are locally stable. However, the global stability of an isolated SWNT should be determined mainly by the competition between the strain introduced by rolling up a planar graphene strip to form the tube and the decrease in energy resulting from the elimination of the dangling bonds along the edges of the strip. The normalized strain energy E_s defined by the difference between the total energy per carbon of the nanotube and that of the graphite sheet, should scale as r^{-2} .^{23,29} On the other hand, the normalized "edge energy" E_e defined by the difference between the total energy per carbon of an extended graphitic strip and that of the graphite sheet, should scale as r^{-1} .^{30,31} Hence, as r decreases E_s will increase more rapidly than E_e , implying the existence of a critical radius r_c such that if $r < r_c$, then the nanotube is unstable with respect to the planar strip ($E_s > E_e$).

Spin-unrestricted results for E_e from relaxed strips are compared to E_s in Fig. 3. Even for narrow SWNT's the translational unit cell of the strip can contain a large number

of atoms given by $N_s = 4(n_1^2 + n_2^2 + n_1 n_2)/L$, where L is the largest common divisor of $2n_1 + n_2$ and $2n_2 + n_1$.¹⁵ Hence, E_e was calculated only for the zigzag tubes. This simplification should not significantly affect the fitting shown in Fig. 3 that results in $r_c = 0.191$ nm. Although this r_c is within the range of predictions based on semiempirical approaches,^{4,30,31} Peng *et al.* observed a SWNT with a radius of 0.165 nm which they suggested was a (4,0) SWNT.⁴ However, because the radius of this tube is near r_c , it could be mechanically stable at room temperature, but energetically unstable with respect to the corresponding strip.⁴ In any event, our calculated value of r_c indicates that the narrow SWNT's found encased in multiwalled tubes^{1,2} and zeolites,³ if isolated, should be stable against complete unzipping along the nanotube axis.

In summary, although many of the narrow SWNT's are stable and can be either semiconductors or metals, their electronic structure near ϵ_F often cannot be understood starting from the graphene sheet model.

This work was supported by ONR both at OSU and NRL. I.C. and J.W.M. also acknowledge support by OSU.

- ¹L.F. Sun, S.S. Xie, W. Liu, W.Y. Zhou, Z.Q. Liu, D.S. Tang, G. Wang, and L.X. Qian, *Nature (London)* **403**, 384 (2000).
- ²L. Qin, X. Zhao, K. Hirahara, Y. Miyamoto, Y. Ando, and S. Iijima, *Nature (London)* **408**, 50 (2000).
- ³N. Wang, Z.K. Tang, G.D. Li, and J.S. Chen, *Nature (London)* **408**, 50 (2000).
- ⁴L.-M. Peng, Z.L. Zhang, Z.Q. Xue, Q.D. Wu, Z.N. Gu, and D.G. Pettifor, *Phys. Rev. Lett.* **85**, 3249 (2000).
- ⁵J.W. Mintmire, B.I. Dunlap, and C.T. White, *Phys. Rev. Lett.* **68**, 631 (1992).
- ⁶S.J. Tans, M.H. Vevoret, H.J. Dai, A. Thess, R.E. Smalley, L.J. Geerligs, and C. Dekker, *Nature (London)* **386**, 474 (1997).
- ⁷J.W.G. Wildoer, L.C. Venema, A.G. Rinzler, R.E. Smalley, and C. Dekker, *Nature (London)* **391**, 59 (1998).
- ⁸T.W. Odom, J.L. Huang, P. Kim, and C.M. Lieber, *Nature (London)* **391**, 62 (1998).
- ⁹P.L. McEuen, M. Bockrath, D.H. Cobden, Y.G. Yoon, and S.G. Louie, *Phys. Rev. Lett.* **83**, 5098 (1999).
- ¹⁰W.J. Liang, M. Bockrath, D. Bozovic, J.H. Hafner, M. Tinkham, and H. Park, *Nature (London)* **411**, 6868 (2001).
- ¹¹S.G. Lemay, J.W. Janssen, M. van den Hout, M. Mooij, M.J. Bronikowski, P.A. Willis, R.E. Smalley, L.P. Kouwenhoven, and C. Dekker, *Nature (London)* **412**, 6847 (2001).
- ¹²M. Ouyang, J.-L. Huang, and C.M. Lieber, *Phys. Rev. Lett.* **88**, 066804 (2002).
- ¹³N. Hamada, S.I. Sawada, and A. Oshiyama, *Phys. Rev. Lett.* **68**, 1579 (1992).
- ¹⁴R. Saito, M. Fujita, G. Dresselhaus, and M.S. Dresselhaus, *Appl. Phys. Lett.* **60**, 2204 (1992).
- ¹⁵C.T. White, D.H. Robertson, and J.W. Mintmire, *Phys. Rev. B* **47**, 5485 (1993).
- ¹⁶J.W. Mintmire, D.H. Robertson, and C.T. White, *J. Phys. Chem. Solids* **54**, 1835 (1993).
- ¹⁷C.T. White and T.N. Todorov, *Nature (London)* **393**, 6682 (1998); **411**, 649 (2001).
- ¹⁸X. Blase, L.X. Benedict, E.L. Shirley, and S.G. Louie, *Phys. Rev. Lett.* **72**, 1878 (1994).
- ¹⁹J.W. Mintmire and C.T. White, *Phys. Rev. Lett.* **50**, 101 (1983); *Phys. Rev. B* **28**, 3283 (1983).
- ²⁰J. W. Mintmire, in *Density Functional Methods in Chemistry*, edited by J. K. Labanowski (Springer-Verlag, Berlin, 1990), p. 125.
- ²¹C. T. White, J. W. Mintmire, R. C. Mowrey, D. W. Brenner, D. H. Robertson, J. A. Harrison, and B. I. Dunlap, in *Buckminsterfullerenes*, edited by W. E. Billups and M. Ciufolini (VCH Publishers, NY, 1993), p. 125.
- ²²J.W. Mintmire and C.T. White, *Phys. Rev. Lett.* **81**, 2506 (1998).
- ²³D.H. Robertson, D.W. Brenner, and J.W. Mintmire, *Phys. Rev. B* **45**, 12 592 (1992).
- ²⁴C. T. White, D. H. Robertson, and J. W. Mintmire, in *Clusters and Nanostructured Materials*, edited by P. Jena and S. N. Behera (Nova Science Publishers, NY, 1996), p. 231.
- ²⁵C.L. Kane and E.J. Mele, *Phys. Rev. Lett.* **78**, 1932 (1997).
- ²⁶M. Ouyang, J.L. Huang, C.L. Cheung, and C.M. Lieber, *Science* **292**, 5517 (2001).
- ²⁷J.W. Mintmire and C.T. White, *Synth. Met.* **77**, 231 (1996).
- ²⁸C.T. White and J.W. Mintmire, *Nature (London)* **394**, 29 (1998).
- ²⁹G.B. Adams, O.F. Sankey, J.B. Page, M. O'Keefe, and D.A. Drabold, *Science* **256**, 1792 (1992).
- ³⁰S. Sawada and N. Hamada, *Solid State Commun.* **83**, 917 (1992).
- ³¹A.A. Lucas, P.H. Lambin, and R.E. Smalley, *J. Phys. Chem. Solids* **54**, 587 (1993).